Talanta 130 (2014) 356–362

Contents lists available at ScienceDirect

Talanta

journal homepage: www.elsevier.com/locate/talanta

Rhodamine-based fluorescent probe for direct bio-imaging of lysosomal pH changes

Xue-Lin Shi [a], Guo-Jiang Mao [c,*], Xiao-Bing Zhang [a,b,**], Hong-Wen Liu [a], Yi-Jun Gong [c], Yong-Xiang Wu [a], Li-Yi Zhou [a], Jing Zhang [a], Weihong Tan [a]

[a] Molecular Science and Biomedicine Laboratory, State Key Laboratory of Chemo/Biosensing and Chemometrics, College of Chemistry and Chemical Engineering, College of Biology, Hunan University, Changsha 410082, PR China
[b] State Key Laboratory of Fine Chemicals, Dalian University of Technology, E224 West Campus 2, Linggong Road, Dalian 116024, PR China
[c] School of Chemistry and Chemical Engineering, Henan Normal University, Xinxiang 453007, PR China

ARTICLE INFO

Article history:
Received 18 April 2014
Received in revised form
3 July 2014
Accepted 10 July 2014
Available online 18 July 2014

Keywords:
Rhodamine-morpholine (**RM**)
Fluorescence probe
Lysosomal pH
Live cells

ABSTRACT

Intracellular pH plays a pivotal role in various biological processes. In eukaryotic cells, lysosomes contain numerous enzymes and proteins exhibiting a variety of activities and functions at acidic pH (4.5–5.5), and abnormal variation in the lysosomal pH causes defects in lysosomal function. Thus, it is important to investigate lysosomal pH in living cells to understand its physiological and pathological processes. In this work, we designed a one-step synthesized rhodamine derivative (**RM**) with morpholine as a lysosomes tracker, to detect lysosomal pH changes with high sensitivity, high selectivity, high photostability and low cytotoxicity. The probe **RM** shows a 140-fold fluorescence enhancement over a pH range from 7.4 to 4.5 with a pK_a value of 5.23. Importantly, **RM** can detect the chloroquine-induced lysosomal pH increase and monitor the dexamethasone-induced lysosomal pH changes during apoptosis in live cells. All these features demonstrate its value of practical application in biological systems.

1. Introduction

Intracellular pH plays a pivotal role in various biological processes, such as cell growth and apoptosis [1–5], ion transport and homeostasis [6–8], drug resistance [9], endocytosis [10,11], and enzymatic activity [12,13]. In eukaryotic cells, lysosomes contain numerous enzymes and proteins exhibiting a variety of activities and functions at acidic pH (4.5–5.5) [14–16]. Abnormal variation in the lysosomal pH causes defects in lysosomal function, which leads to lysosomal storage diseases [17], cancer [18,19], and Alzheimer's disease [20–22]. Importantly, the gradient decay of lysosomal proton during apoptosis process seems to cause the acidification of the cytosol and lysosomal pH increase [23], which would be used for monitoring apoptosis. Thus, it is important to investigate lysosomal pH in living cells to understand its physiological and pathological processes.

In recent years, fluorescent probes [24–31], nanoparticles [32–35] and polymers [36,37] have been widely used for measuring pH changes in solutions or live cells. Among them, fluorescent probes have attracted particular interest by virtue of its high sensitivity, real-time spatial imaging and non-damaging detection of targets in living cells or tissues [38–40]. Although some of them have been applied to subcellular pH sensing, only a limited number of probes based on rhodamine derivatives can track pH changes in the lysosome [25,41–44,48–54]. Moreover, most of such lysosomal pH probes suffered from severe disadvantages, including complicated synthesis route [44,49], low sensitivity [50,53,54], interferences from other species [49,52,53], and the short-wavelength emission which is not beneficial for bio-imaging [44]. Therefore, it is still essential to develop an easy-synthesized lysosome-targetable pH fluorescent probe with high sensitivity and selectivity.

Rhodamine dyes have been extensively used as fluorophores by virtue of their excellent photophysical properties [55–59], such as high extinction coefficients, excellent quantum yields, great photostability, and relatively long emission wavelengths. More importantly, the rhodamine with a ring-closed spirolactam unit has been reported to show H^+-triggered "turn-on" fluorescence signals. Based on this mechanism, some pH fluorescence probes have been developed for measuring pH changes [45–54]. On the other hand, morpholine has been reported as a lysosomes tracker [60–62], and so we envisioned that a more convenient and sensitive lysosomal pH probe might be achieved if we introduced a morpholine into a ring-closed rhodamine derivative. Based on these two points,

* Corresponding author. Tel.: +86 373 3326335.
** Corresponding author. Tel./fax: +86 731 88821894.
E-mail addresses: mgz1985419@163.com (G.-J. Mao), xbzhang@hnu.edu.cn (X.-B. Zhang).

http://dx.doi.org/10.1016/j.talanta.2014.07.030
0039-9140/

we designed a new rhodamine-morpholine (**RM**) fluorescent probe to detect lysosomal pH changes in this work. In our novel probe **RM**, a 4-(2-aminoethyl) morpholine was chosen as an important reactant, in which the amino group was utilized to construct the rhodamine spirolactam ring-closed form as a pH sensitive module and the morpholine was introduced as a lysosomes-targeting unit [60–62]. To the best of our knowledge, morpholine as a lysosomes tracker has never been used to develop a lysosomal pH fluorescent probe, and so we investigated the analytical performances of the probe **RM** such as sensitivity, selectivity, photostability, and cytotoxicity, which demonstrated its value of practical application in biological systems.

2. Experimental section

2.1. Reagents and apparatus

All chemicals were obtained from commercial suppliers and used without further purification. Water used in all experiments was doubly distilled and purified by a Milli-Q system (Millipore, USA). Mass spectra were performed using an LCQ Advantage ion trap mass spectrometer (Thermo Finnigan). NMR spectra were recorded on a Bruker DRX-400 spectrometer using TMS as an internal standard. All chemical shifts are reported in the standard δ notation of parts per million. Thin layer chromatography (TLC) was carried out using silica gel 60 F254, and column chromatography was conducted over silica gel (100–200 mesh), both of them were obtained from Qingdao Ocean Chemicals (Qingdao, China). The pH was measured with a Mettler-Toledo Delta 320 pH meter. Fluorescence measurements were carried out on a Hitachi-F4500 fluorescence spectrometer with excitation and emission slits set at 5.0 nm and 10.0 nm respectively. Fluorescence images of MCF-7 cells were obtained using OLYMPUS FV-1000 inverted fluorescence microscope.

2.2. Synthesis of compound RM

Rhodamine B (0.6 g, 1.3 mmol) and 4-(2-aminoethyl)-morpholine (0.26 g, 2 mmol) were dissolved in ethanol (50 mL), and the solution was refluxed for 8 h. After the solution was cooled to room temperature, the solution was concentrated under reduced pressure and the residue was purified by the silica gel chromatography (CH_2Cl_2/CH_3OH =25:1, v/v) to afford compound **RM** as a white solid (0.35 g, 49%). ^{1}H NMR (DMSO-d_6, 400 MHz) δ (ppm): 7.763–7.784 (m, 1H), 7.495–7.521 (m, 2H), 7.031–7.051 (m, 1H), 6.298–6.384 (m, 6H), 3.396–3.418 (t, J=4.4 Hz, 2H), 3.293–3.339 (q, 8H), 3.057–3.093 (t, J=7.6 Hz, 2H), 2.062 (s, 4H), 1.878–1.914 (t, J=6.8 Hz, 2H), 1.057–1.091 (t, J=6.8 Hz, 12H). MS (ESI) m/z 555.4 $(M+1)^+$.

2.3. Spectrophotometric experiments

The fluorescence measurement experiments were measured in buffered (40 mM Britton–Robinson buffer solution) aqueous DMSO (as co-solvent) solution (H_2O/DMSO=99:1, v/v). The pH of Britton–Robinson buffer solution used was between 4 and 7.4, which was achieved by adding minimal volumes of HCl or NaOH. The fluorescence emission spectra were recorded at excitation wavelength of 525 nm with emission wavelength range from 550 to 650 nm. A 1×10^{-3} M stock solution of **RM** was prepared by dissolving **RM** in dimethyl sulphoxide (DMSO). Procedure of calibration measurements with **RM** in the buffer with different pH was as follows: 20 μL stock solution of **RM** and 1980 μL Britton–Robinson buffer solution with different pH were combined to afford a test solution, which contained 10×10^{-6} M of **RM**. The solutions of various testing species were prepared from $NaNO_3$, NaBr, $NaH_2PO_4\cdot2H_2O$, NaAc, KI, Na_2CO_3, Na_2SO_4, $Na_2HPO_4\cdot12H_2O$, NaCl, KCl, KNO_3, $CaCl_2$, $MgSO_4$, $Co(CH_3COO)_2\cdot4H_2O$, $CuCl_2\cdot2H_2O$, $Ba(NO_3)_2$, $NiCl_2\cdot6H_2O$, $CrCl_3\cdot6H_2O$, $Zn(NO_3)_2\cdot6H_2O$, $CdCl_2\cdot5/2H_2O$, $Al(NO_3)_3\cdot9H_2O$, $Mn(CH_3COO)_2\cdot4H_2O$ and $Fe(NO_3)_3\cdot9H_2O$ using twice-distilled water with final concentrations of 0.0125 M for them, as well as, glutathione (GSH), cysteine (Cys), homocysteine (Hcy), arginine (Arg), valine (Val), tryptophan (Trp) and glutamate (Glu) using twice-distilled water with final concentrations of 0.025 M for them. Procedure of selectivity experiments was as follows: for cations or anions, 20 μL stock solution of **RM**, 1948 μL Britton–Robinson buffer solution (pH=5) and 32 μL solution of each cation or anion were combined to afford a test solution, which contained 10×10^{-6} M of **RM** and 200 μM cation or anion; for amino acids, 20 μL stock solution of **RM**, 1900 μL Britton–Robinson buffer solution (pH=5) and 80 μL solution of each amino acid were combined to afford a test solution, which contained 10×10^{-6} M of **RM** and 1 mM amino acid.

2.4. Cell culture and imaging experiments

The living MCF-7 cells were provided by the Biomedical Engineering Center of Hunan University (China). Immediately before the experiments, the cells were washed with Dulbecco's phosphate buffered saline (DPBS), followed by incubating with **RM** (10 μM) for 30 min (in DPBS containing 0.2% DMSO) at 37 °C, then by washing with DPBS three times and imaged. LysoSensorTM Green DND-189 (1 μM, Invitrogen) was used to co-stain the cells to lysosome. Chloroquine (100 μM) was added to induce lysosomal pH change, and dexamethasone (2 μM) was added to induce lysosomal pH change during apoptosis. Fluorescence microscopy imaging of MCF-7 cells was observed under an Olympus FV1000 laser confocal microscope. Excitation wavelength of the laser was 543 nm. Emissions were between 550–650 nm.

2.5. Photostability test

MCF-7 cells were incubated with **RM** (10 μM) for 30 min. The cells were then washed three times with DPBS, exposed to laser illumination (λ_{ex}=543 nm), and then imaged for 20 min.

2.6. Cytotoxicity experiments

The cytotoxic effects of probe **RM** were assessed using the MTT assay [63]. Briefly, MCF-7 cells were seeded in 96-well microplates (Nunc, Denmark) at a density of 1×10^5 cells/mL in 100 μL of medium containing 10% fetal bovine serum (FBS). After 24 h of cell attachment, the plates were washed with 100 μL/well DPBS. The cells were then cultured in a medium with 10 μM **RM** for 12 h. Cells in a culture medium without fluorescent dyes were used as the control. Six replicate wells were used for each control and test concentration. MTT (10 μL, 5 mg/mL) in DPBS was subsequently added to each well. The plates were then incubated at 37 °C for 4 h in a 5% CO_2 humidified incubator. The medium was carefully removed, and the purple products were lysed in 200 μL DMSO. The plate was shaken for 10 min, and the absorbance was measured at 570 nm using a microplate reader (Thermo Fisher Scientific). Cell viability was expressed as a percentage of the control culture value.

3. Results and discussion

3.1. Optimized design and synthesis of probe RM for lysosomal pH

In recent years, some lysosomal pH probes based on rhodamine derivatives have been developed [49,50,52–54]. In 2012, the Peng group reported a rhodamine derivative with a methylcarbitol

group for imaging lysosomal pH with a 50-fold fluorescence enhancement, which showed a moderate sensitivity over a pH range from 7.4 to 4.5 [50]. Next, the Miao group reported a new rhodamine B-based lysosomal pH fluorescent indicator, **RCE**. The probe **RCE** exhibited an excellent analytical performance for lysosomal pH, but it suffered interferences from other species such as Cu^{2+}, Co^{2+} and Lysine [52]. In 2013, the Miao group reported another new fluorescent pH probe for imaging lysosomes, but the probe showed a low sensitivity with only a 20-fold fluorescence enhancement over a pH range from 7.5 to 4.1 and suffered interferences from metal ions such as Cu^{2+}, Co^{2+}, Zn^{2+} and Al^{3+} [54]. In 2014, the Han group reported a rhodamine–benzimidazole-based probe for imaging of lysosomal pH. However, the reported probe also showed a low fluorescence enhancement and suffered slight interferences from metal ions such as Fe^{3+} [53]. To obtain a lysosomal pH fluorescent probe with improved sensitivity and selectivity, a lysosome-targetable pH fluorescent probe, **RM** has been developed. We designed the probe with two considerations. Firstly, rhodamine B was chosen as a fluorophore by virtue of its excellent photophysical properties. Furthermore, the rhodamine B derivatives with a spirolactam ring have been reported to show H^+-triggered "turn-on" fluorescence signals. On the other hand, in order to achieve lysosome-targetability, 4-(2-aminoethyl)-morpholine was attached to the rhodamine fluorophore, which can help the probe to accumulate selectively in lysosomes. The specific localization of aminoethyl morpholine in lysosomes has been proved by some recent reports [60–62].

Compound **RM** was efficiently synthesized following the synthetic methodology shown in Scheme 1, with Rhodamine B and 4-(2-aminoethyl)-morpholine as initial material. The probe was characterized using ^{1}H NMR and MS (Figs. S1 and S2).

3.2. Fluorescent analytical performance of probe RM

The fluorescence responses of the probe **RM** at various pH were recorded at an excitation wavelength of 525 nm, with results illustrated in Fig. 1a. **RM** was almost nonfluorescent at pH 7.4 because of its stable "ring-closed" form. However, the fluorescence intensity of **RM** was significantly enhanced as the H^+ concentration was increased to induce the spirolactam ring open. It shows a 140-fold increase in the emission intensities within the pH range of 7.4–4.5. In Fig. 1b, the analysis of fluorescence intensity changes as a function of pH by using the Henderson–Hasselbalch equation [64]: $\log[(I_{max}-I)/(I-I_{min})]=pH-pK_a$, where I is the observed fluorescence intensity, I_{max} and I_{min} are the corresponding maximum and minimum respectively, yielded a pK_a of 5.23, which is valuable for studying lysosomal pH. Moreover, **RM** can respond to H^+ quickly and its fluorescence intensity saturation is reached within several seconds at pH 4.50 and 5.00, which is vital to detect lysosomal pH changes in real time.

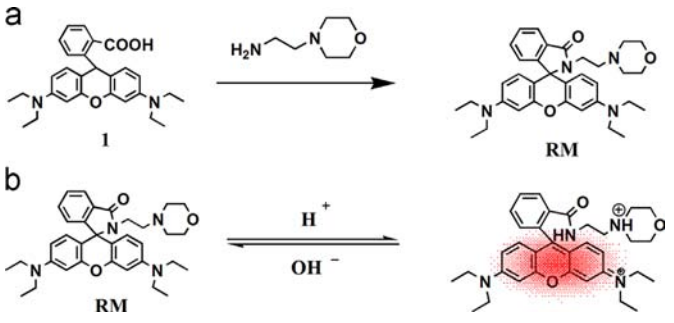

Scheme 1. Structure and synthetic route of **RM** and its response mechanism to pH.

Besides sensitivity, selectivity is another very important parameter to evaluate the performance of a new fluorescent probe. Particularly, for a bio-imaging probe with potential application

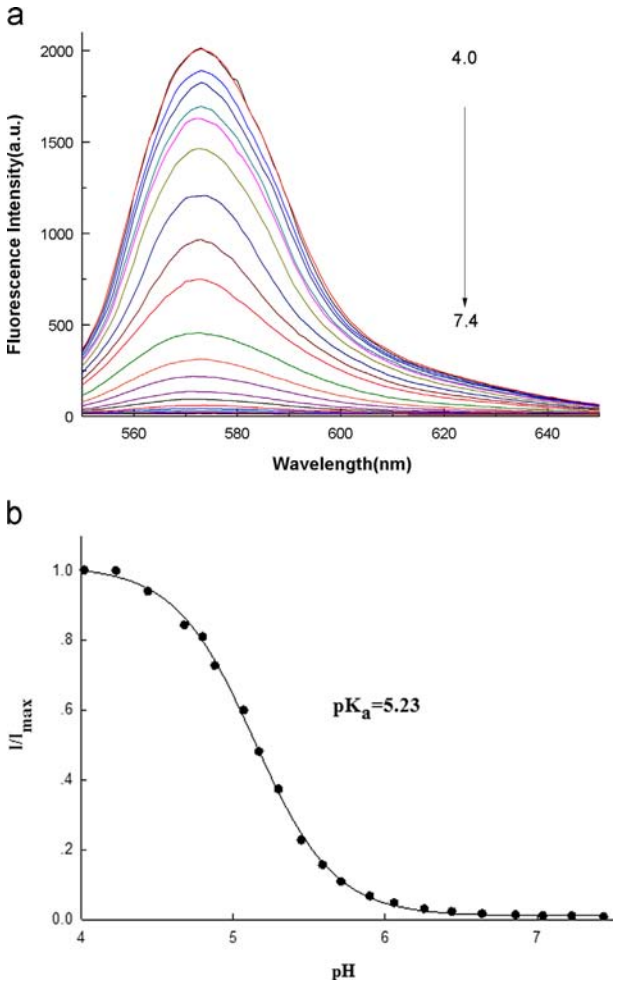

Fig. 1. (a) Fluorescence spectra of **RM** (10 μM) at various pH in Britton–Robinson buffer solution (40 mM), λ_{ex}=525 nm. (b) pH titration curve of **RM**, λ_{ex}=525 nm, λ_{em}=573 nm.

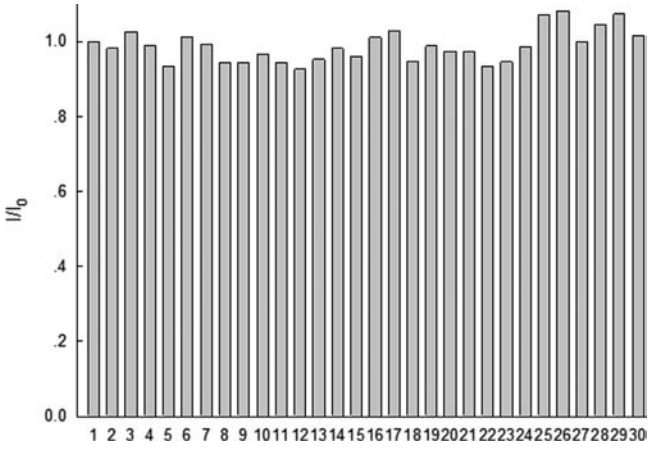

Fig. 2. Fluorescence intensity of **RM** in the presence of miscellaneous ions in Britton–Robinson buffer solution at pH 5.00. From left to right: H^+, Na^+, K^+, Ca^{2+}, Mg^{2+}, Zn^{2+}, Cu^{2+}, Fe^{3+}, Al^{3+}, Mn^{2+}, Ni^{2+}, Co^{2+}, Cd^{2+}, NO_3^-, Cl^-, Br^-, I^-, CO_3^{2-}, SO_4^{2-}, $H_2PO_4^-$, HPO_4^{2-}, PO_4^{3-} and Ac^- were 200 μM. Arg, Val, Trp, Glu, Cys, GSH and Hcy were 1 mM. Condition: excitation wavelength is 525 nm, emission wavelength is 573 nm.

in complex biological samples, a highly selective response to the target specie over other potentially competing species is necessary. As shown in Fig. 2, the selectivity experiments of **RM** were extended to 29 kinds of other biological-related species. The responses of **RM** were found to be highly selective for H^+ (pH=5) in the presence of common cations, anions or amino acids. The fluorescence intensity of **RM** (10 μM) did not obviously changed upon the addition of 20 equiv of biologically relevant metal ions (200 μM), i.e., Na^+, K^+, and Ca^{2+} and 20 equiv of other transition metal ions (Mn^{2+}, Ni^{2+}, Co^{2+} and Cd^{2+}). Moreover, various common anions (NO_3^-, Cl^-, Br^-, I^-, CO_3^{2-}, SO_4^{2-}, $H_2PO_4^-$, HPO_4^{2-}, PO_4^{3-} and Ac^-) exhibited negligible interference on the responses of **RM** to H^+. In the presence of 1 mM of biologically relevant amino acids including GSH, Cys, Hcy, Arg, Val, Trp, and Glu, the fluorescence intensity of **RM** remained generally stable also. The results reveal that the H^+-induced fluorescence response was unaffected by the other species, which indicate that the probe **RM** has a highly specific selectivity for H^+. Most notably, the probe displayed an excellent reversibility. In Fig. 3, it showed the fluorescence intensity changes of **RM** when the pH is switched between 4.57 and 7.43 three times, and approximately 92.5% of the original signal was successfully generated.

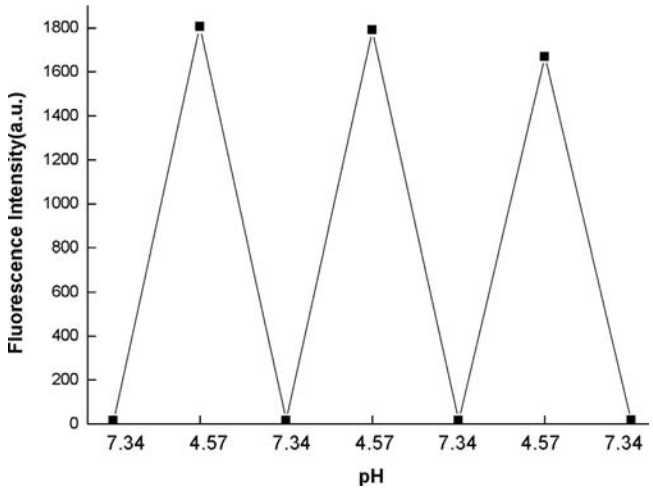

Fig. 3. Fluorescence intensity of **RM** in Britton–Robinson buffer solution. pH was changed repeatedly between 4.57 and 7.34. Conditions: excitation wavelength is 525 nm, emission wavelength is 573 nm.

3.3. Co-localization experiments to lysosomes

The acidity of the lysosome (pH 4.5–5.5) is vital to the optimal activities of various hydrolases. Next we applied **RM** in living cells to assess the ability of the probe **RM** for localizing the lysosomes. The MCF-7 cells were co-stained with **RM** and LysoSensor Green DND-189 which is a commercially available lysosome-specific staining probe. As shown in Fig. 4, the confocal fluorescence microscopy results showed that **RM** exhibited observable red punctate fluorescence near the perinuclear regions of live MCF-7 cells. The co-localization of **RM** with LysoSensor Green was observed with high overlaps, which suggest that **RM** selectively stains lysosomes in live cells.

3.4. Photostability of probe RM for lysosomal pH

Photostability is one of the most important criteria for developing fluorescent imaging dyes, which adversely affects the temporal monitoring of dynamic events in cells. Thus, we investigated the photostability of **RM** in the live MCF-7 cells. As shown in Fig. 5, the MCF-7 cells co-stained with **RM** exhibited similar fluorescence intensity at different time throughout the cells was exposed to laser illumination for 20 min, which indicates the high photostability of **RM** under biological conditions.

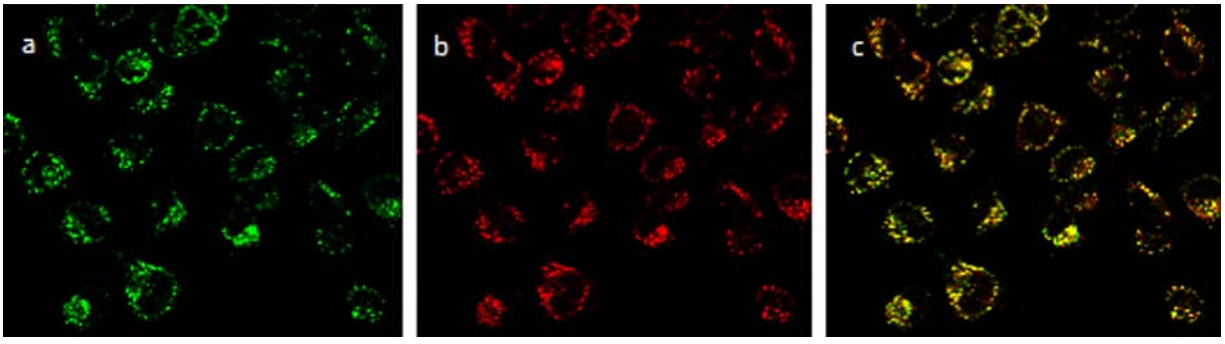

Fig. 4. Cells were stained with: (a) 1 μM LysoSensor Green, (b) 10 μM **RM**. (c) areas of colocalization appear in yellow. **RM** and LysoSensor Green were excited at 543 nm and 488 nm, respectively. The fluorescence images were recorded at 550–650 nm and 495–515 nm.

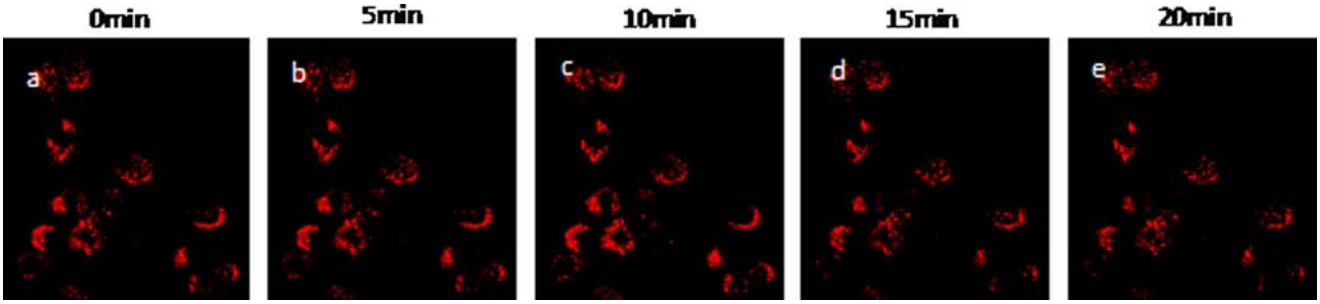

Fig. 5. Photostability of **RM** in MCF-7 cells illuminated with a laser. (a)–(e) Confocal fluorescence images of **RM** at various time points.

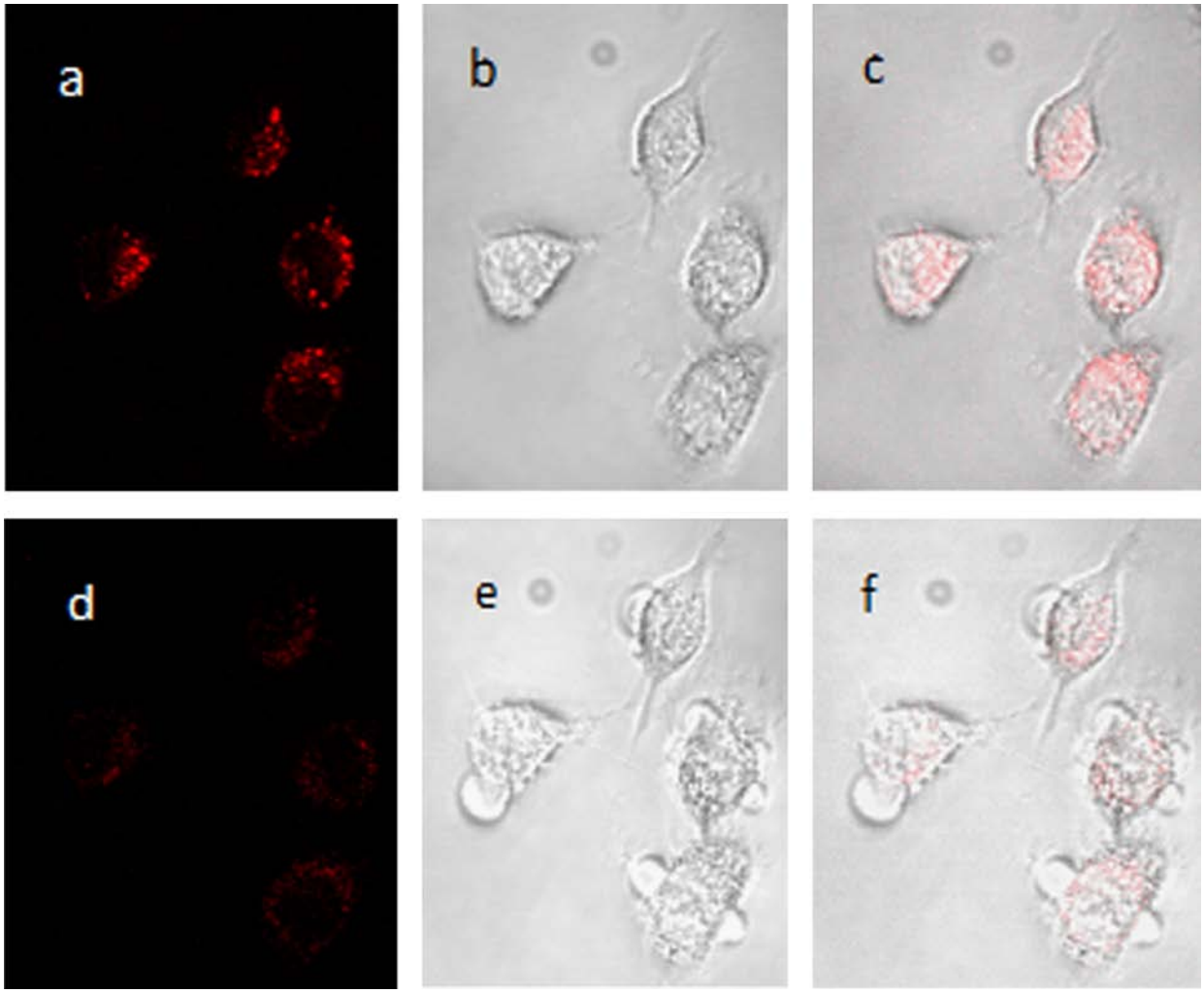

Fig. 6. Fluorescence images of **RM** in MCF-7 cells stimulated with chloroquine. (a–c) Images of the stained cells before chloroquinest simulation; (d–f) images of cells in (a–c) exposed to 100 μM chloroquine for 2 min. The probe was excited at 543 nm and the fluorescence was collected at 550–650 nm.

3.5. Lysosomal pH tracking in chloroquine-treated MCF-7 cells

In order to prove that the probe **RM** can track lysosomal pH changes under different acidic conditions in cells, we made the following experiment. MCF-7 cells were first cultivated with **RM** (10 μM) for 30 min, which showed a strong fluorescence at this time. And then the same MCF-7 cells were treated with the antimalaria drug chloroquine, which is a cell-permeable base and can neutralize the acidic environment in lysosomes, thus leading to an increase in lysosomal pH [65]. With addition of chloroquine (100 μM), the fluorescence intensities were clearly reduced after 2 min (Fig. 6). This result indicates that **RM** can detect lysosomal pH changes in real time.

3.6. Lysosomal pH tracking during apoptosis

It is known that the lysosomal pH shows an increase during apoptosis, which might be due to lysosomal proton release [23,50]. In order to further prove that the probe **RM** can track lysosomal pH changes in cells, **RM** was applied to monitor lysosomal pH changes during apoptosis in live cells. MCF-7 cells were first cultivated with **RM** (10 μM) for 30 min, which showed a strong fluorescence at this time. And then the same MCF-7 cells were treated with the drug dexamethasone, which can induce apoptosis in live cells. After the dexamethasone (2 μM) was added, the fluorescence intensity of MCF-7 cells exhibited time-dependent decreases due to the increase of the lysosomal pH induced by apoptosis which was proved by dramatically morphological changes of the cells (Fig. 7). The result is consistent with the previous studies [50,66] and further proves that the probe **RM** can indeed image lysosomal pH changes in real time.

3.7. Cytotoxicity experiments

To assess the biological compatibility of the **RM** probe, cytotoxicity experiments were carried on. MTT assays indicated that MCF-7 cells viabilities were not affected by incubation with 10 μM **RM** for 12 h. These results demonstrate that the probe **RM** has a high biological compatibility and it is suitable for imaging of the lysosomal pH changes.

4. Conclusions

In summary, we have reported a new rhodamine–morpholine (**RM**) fluorescent probe for monitoring of lysosomal pH changes in live cells, which has high sensitivity and selectivity, as well as high photostability and low cytotoxicity. The fluorescence intensity of **RM** is sensitive to acidic pH in a short response time with a pK_a value of 5.23. It shows a 140-fold increase in the emission intensities within the pH range of 7.4–4.5 due to the H^+-triggered "turn-on" fluorescence signal. Importantly, **RM** was successfully

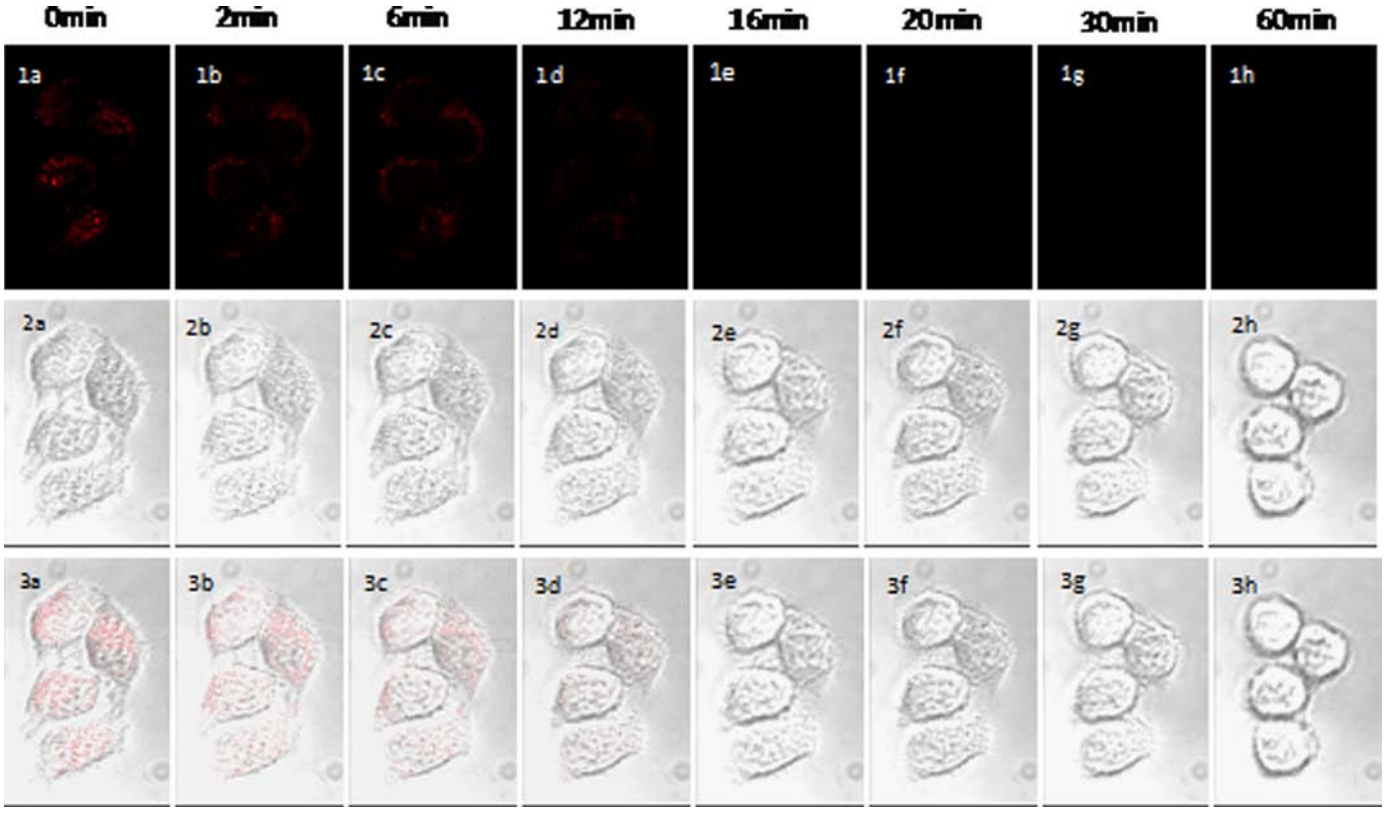

Fig. 7. Time dependent fluorescence changes of **RM** in MCF-7 cells undergoing apoptotic death. a, b, c, d, e, f, g and h indicated times of 0, 2, 6, 12, 16, 20, 30 and 60 min, respectively. 1, 2 and 3 represent red channel image (λ_{ex}=543 nm, λ_{em}=550–650 nm), bright field and overlap of 1 and 2, respectively.

applied to detect the chloroquine-induced increase in lysosomal pH and monitor the lysosomal pH changes during apoptosis in live cells, demonstrating its value of practical application in biological systems.

Acknowledgment

This work was supported by the National Key Scientific Program of China (2011CB911000), NSFC (Grants 21325520, 21327009, J1210040, 21177036), the Foundation for Innovative Research Groups of NSFC (Grant 21221003), the National Natural Science Foundation of China (21135001), the National Instrumentation Program (2011YQ030124), State Key Laboratory of Fine Chemicals Dalian at University of Technology (KF1301) and the Hunan Provincial Natural Science Foundation (Grant 11JJ1002).

Appendix A. Supporting information

Supporting information associated with this article can be found in the online version at http://dx.doi.org/10.1016/j.talanta.2014.07.030.

References

[1] D. Perez-Sala, D. Collado-Escobar, F. Mollinedo, J. Biol. Chem. 270 (1995) 6235–6242.
[2] A. Ishaque, M. Al-Rubeai, J. Immunol. Methods 221 (1998) 43–57.
[3] R.A. Gottlieb, A. Dosanjh, Proc. Natl. Acad. Sci. USA 93 (1996) 3587–3591.
[4] R.A. Gottlieb, J. Nordberg, E. Skowronski, B.M. Babior, Proc. Natl. Acad. Sci. USA 93 (1996) 654–658.
[5] R.A. Gottlieb, H.A. Giesing, J.Y. Zhu, R.L. Engler, B.M. Babior, Proc. Natl. Acad. Sci. USA 92 (1995) 5965–5968.
[6] K.R. Hoyt, I.J. Reynolds, J. Neurochem. 71 (1998) 1051–1058.
[7] T. Speake, A.C. Elliott, J. Physiol. 506 (1998) 415–430.
[8] R.G.W. Anderson, L.J. Orci, Cell Biol. 106 (1988) 539–543.
[9] S. Simon, D. Roy, M. Schindler, Proc. Natl. Acad. Sci. USA 91 (1994) 1128–1132.
[10] M. Miksa, H. Komura, R. Wu, K.G. Shah, P. Wang, J. Immunol. Methods 342 (2009) 71–77.
[11] M. Lakadamyali, M.J. Rust, H.P. Babcock, X. Zhuang, Proc. Natl. Acad. Sci. USA 100 (2003) 9280–9285.
[12] V.A. Golovina, M.P. Blaustein, Science 275 (1997) 1643–1648.
[13] R.T. Kennedy, L. Huang, C.A. Aspenwall, J. Am. Chem. Soc. 118 (1996) 1795–1796.
[14] S. Kornfeld, I. Mellman, Annu. Rev. Cell Biol. 5 (1989) 483–525.
[15] E.J. Blott, G.M. Griffiths, Nat. Rev. Mol. Cell Biol. 3 (2002) 122–131.
[16] J. Stinchcombe, G. Bossi, G.M. Griffiths, Science 305 (2004) 55–59.
[17] T. Fukuda, L. Ewan, M. Bauer, R.J. Mattaliano, K. Zaal, E. Ralston, P.H. Plotz, N. Raben, Ann. Neurol. 59 (2006) 700–708.
[18] M. Schindler, S. Grabski, E. Hoff, S. Simon, Biochemistry 35 (1996) 2811–2817.
[19] H. Izumi, T. Torigoe, H. Ishiguchi, H. Uramoto, Y. Yoshida, M. Tanabe, T. Ise, T. Murakami, T. Yoshida, M. Nomoto, K. Kohno, Cancer Treat. Rev. 29 (2003) 541–549.
[20] D.A. Russell, R.H. Pottier, D.P. Valenzeno, Photochem. Photobiol. 59 (1994) 309–313.
[21] T.A. Davies, R.E. Fine, R.J. Johnson, C.A. Levesque, W.H. Rathbun, K.F. Seetoo, S.J. Smith, G. Strohmeier, L. Volicer, L. Delva, Biochem. Biophys. Res. Commun. 194 (1993) 537–543.
[22] H.S. Mogensen, D.M. Beatty, S.J. Morris, O.S. Jorgensen, Neuroreport 9 (1998) 1553–1558.
[23] C. Nilsson, K. Kagedal, U. Johansson, K. Öllinger, Methods Cell Sci. 25 (2004) 185–194.
[24] H.M. Kim, M.J. An, J.H. Hong, B.H. Jeong, O. Kwon, J.Y. Hyon, S.C. Hong, K.J. Lee, B.R. Cho, Angew. Chem. Int. Ed. 47 (2008) 2231–2234.
[25] H.J. Kim, C.H. Heo, H.M. Kim, J. Am. Chem. Soc. 135 (2013) 17969–17977.
[26] H.J. Park, C.S. Lim, E.S. Kim, J.H. Han, T.H. Lee, H.J. Chun, B.R. Cho, Angew. Chem. Int. Ed. 51 (2012) 2673–2676.
[27] T. Myochin, K. Kiyose, K. Hanaoka, H. Kojima, T. Terai, T. Nagano, J. Am. Chem. Soc. 133 (2011) 3401–3409.
[28] B. Tang, F. Yu, P. Li, L. Tong, X. Duan, T. Xie, X. Wang, J. Am. Chem. Soc. 131 (2009) 3016–3023.
[29] M. Lee, N.G. Gubernator, D. Sulzer, D. Sames, J. Am. Chem. Soc. 132 (2010) 8828–8830.
[30] J. Han, A. Loudet, R. Barhoumi, R.C. Burghardt, K. Burgess, J. Am. Chem. Soc. 131 (2009) 1642–1643.

[31] U.C. Saha, K. Dhara, B. Chattopadhyay, S.K. Mandal, S. Mondal, S. Sen, M. Mukherjee, S.V. Smaalen, P. Chattopadhyay, Org. Lett. 13 (2011) 4510–4513.
[32] X. Wang, J.A. Stolwijk, T. Lang, M. Sperber, R.J. Meier, J. Wegener, O.S. Wolfbeis, J. Am. Chem. Soc. 134 (2012) 17011–17014.
[33] L.K. Truman, S. Comby, T. Gunnlaugsson, Angew. Chem. Int. Ed. 51 (2012) 9624–9627.
[34] W. Shi, X. Li, H. Ma, Angew. Chem. Int. Ed. 51 (2012) 6432–6435.
[35] M.J. Marín, F. Galindo, P. Thomas, D.A. Russell, Angew. Chem. Int. Ed. 51 (2012) 9657–9661.
[36] H. Peng, J.A. Stolwijk, L. Sun, J. Wegener, Otto. S. Wolfbeis, Angew. Chem. Int. Ed. 49 (2010) 4246–4249.
[37] J. Madsen, I. Canton, N.J. Warren, E. Themistou, A. Blanazs, B. Ustbas, X. Tian, R. Pearson, G. Battaglia, A.L. Lewis, S.P. Armes, J. Am. Chem. Soc. 135 (2013) 14863–14870.
[38] E.L. Que, D.W. Domaille, C.J. Chang, Chem. Rev. 108 (2008) 1517–1549.
[39] O. Thoumine, H. Ewers, M. Heine, L. Groc, R. Frischknecht, G. Giannone, C. Poujol, P. Legros, B. Lounis, L. Cognet, D. Choquet, Chem. Rev. 108 (2008) 1565–1587.
[40] Y. Yang, Q. Zhao, W. Feng, F. Li, Chem. Rev. 113 (2013) 192–270.
[41] D.G. Smith, B.K. McMahon, R. Pala, D. Parker, Chem. Commun. 48 (2012) 8520–8522.
[42] G. Li, D. Zhu, L. Xue, H Jiang, Org. Lett. 15 (2013) 5020–5023.
[43] S. Chen, Y. Hong, Y. Liu, J. Liu, C.W.T. Leung, M. Li, R.T.K. Kwok, E. Zhao, J.W.Y. Lam, Y. Yu, B.Z. Tang, J. Am. Chem. Soc. 135 (2013) 4926–4929.
[44] L. Chen, J. Li, Z. Liu, Z. Ma, W. Zhang, L. Du, W. Xu, H. Fang, M. Li, RSC Adv. 32 (2013) 13412–13416.
[45] L. Yuan, W. Lin, Z. Cao, J. Wang, B. Chen, Chem. Eur. J. 18 (2012) 1247–1255.
[46] M. Tian, X. Peng, J. Fan, J. Wang, S. Sun., Dyes Pigm. 95 (2012) 112–115.
[47] Q.A. Best, R. Xu, M.E. McCarroll, L. Wang, D.J. Dyer, Org. Lett. 12 (2010) 3219–3221.
[48] M.H. Lee, J.H. Han, J.H. Lee, N. Park, R. Kumar, C. Kang, J.S. Kim, Angew. Chem. Int. Ed. 52 (2013) 6206–6209.
[49] J. Fan, C. Lin, H. Li, P. Zhan, J. Wang, S. Cui, M. Hu, G. Cheng, X. Peng., Dyes Pigm. 99 (2013) 620–626.
[50] H. Zhu, J. Fan, Q. Xu, H. Li, J. Wang, P. Gao, X. Peng, Chem. Commun. 48 (2012) 11766–11768.
[51] Z. Li, S. Wu, J. Han, S. Han, Analyst 136 (2011) 3698–3706.
[52] H.S. Lv, S.Y. Huang, B.X. Zhao, J.Y. Miao, Anal. Chim. Acta 788 (2013) 177–182.
[53] Z. Xue, M. Chen, J. Chen, J. Han, S. Han, RSC Adv. 33 (2014) 374–378.
[54] H.S. Lv, S.Y. Huang, Y. Xu, X. Dai, J.Y. Miao, B.X. Zhao, Bioorg. Med. Chem. Lett. 24 (2014) 535–538.
[55] X. Chen, T. Pradhan, F. Wang, Chem. Rev. 112 (2012) 1910–1956.
[56] Y. Yang, Q. Zhao, W. Feng, Chem. Rev. 113 (2013) 192–270.
[57] Y.J. Gong, X.B. Zhang, C.C. Zhang, A.L. Luo, Anal. Chem. 24 (2012) 10777–10784.
[58] Y.J. Gong, X.B. Zhang, Z. Chen, Y. Yuan, Z. Jin, Analyst 137 (2012) 932–938.
[59] A.L. Luo, Y.J. Gong, Y. Yuan, J. Zhang, Talanta 117 (2013) 326–332.
[60] H. Yu, Y. Xiao, L. Jin, J. Am. Chem. Soc. 134 (2012) 17486–17489.
[61] L. Wang, Y. Xiao, W. Tian, L. Deng, J. Am. Chem. Soc. 135 (2013) 2903–2906.
[62] T. Liu, Z. Xu, D.R. Spring, J. Cui, Org. Lett. 15 (2013) 2310–2313.
[63] T. Mosmann, J. Immunol. Methods 65 (1983) 55–63.
[64] L.J. Henderson, Am. J. Physiol. 21 (1908) 173–179.
[65] B. Poole, S.J. Ohkuma, Cell Biol. 90 (1981) 665–669.
[66] K. Kagedal, M. Zhao, I. Svensson, U.T. Brunk, Biochem. J. 359 (2001) 335–343.